



HAL
open science

Controlled release of riboflavin encapsulated in pea protein microparticles prepared by emulsion-enzymatic gelation process

Attaf Djoullah, Rémi Saurel

► **To cite this version:**

Attaf Djoullah, Rémi Saurel. Controlled release of riboflavin encapsulated in pea protein microparticles prepared by emulsion-enzymatic gelation process. *Journal of Food Engineering*, 2021, 292, pp.110276. 10.1016/j.jfoodeng.2020.110276 . hal-03122505

HAL Id: hal-03122505

<https://institut-agro-dijon.hal.science/hal-03122505>

Submitted on 22 Aug 2022

HAL is a multi-disciplinary open access archive for the deposit and dissemination of scientific research documents, whether they are published or not. The documents may come from teaching and research institutions in France or abroad, or from public or private research centers.

L'archive ouverte pluridisciplinaire **HAL**, est destinée au dépôt et à la diffusion de documents scientifiques de niveau recherche, publiés ou non, émanant des établissements d'enseignement et de recherche français ou étrangers, des laboratoires publics ou privés.



Distributed under a Creative Commons Attribution - NonCommercial 4.0 International License

1 **Controlled release of riboflavin encapsulated in pea protein** 2 **microparticles prepared by emulsion-enzymatic gelation process**

3 Attaf Djoullah^{ab}, Rémi Saurel^{a*}

4 *corresponding author.

5 ^a Univ. Bourgogne Franche-Comté, AgroSup Dijon, PAM UMR A 02.102, F-21000 Dijon,
6 France.

7 ^b Département de technologie alimentaire, Unité de Recherche et Développement de
8 l'Intendance, 16000 Alger, Algeria

9 **Abstract**

10 Riboflavin was encapsulated in pea protein microparticles crosslinked by transglutaminase
11 and the release properties of this system was studied in simulated gastric (pH=1.2) and
12 intestinal (pH=7.4) fluids. The microparticles were obtained from a water-in-oil emulsion **and**
13 **subsequent** enzymatic gelation. In presence of polyglycerol polyricinoleate as hydrophobic
14 surfactant, magnetic agitation was preferred to high-speed homogenization in order to form
15 spherical microparticles of ~150 µm average size. The encapsulation **efficiency** of crystallized
16 riboflavin (RF) varied from 74% to 84% depending on the amount of loaded RF (0.1-1.0
17 wt%). According to the kinetic power law model, the release mechanisms of riboflavin **under**
18 **simulated** gastrointestinal conditions were governed by diffusion in absence of digestive
19 enzymes and by a support degradation phenomenon in **their** presence. The designed
20 microparticles **represented** a potential system for the delivery of riboflavin **up to** the intestinal
21 digestion phase.

22

23 **Keywords** : riboflavin, pea proteins, emulsion, transglutaminase, encapsulation, release

24

25 **1. Introduction**

26 The encapsulation of active substances is one of the major innovation challenges in the
27 pharmaceutical, cosmetic and food industries. Encapsulation is a technology that can be
28 applied to a large number of bioactive molecules (antioxidants, vitamins, probiotics, minerals)
29 and **aims** to protect or isolate them from adverse environments, or **allows to** control the
30 release of the encapsulated substances in the gastrointestinal tract ([Đorđević et al, 2015](#)).

31 In food systems, many of these molecules have low solubility, are sensitive to environmental
32 factors (such as light, temperature and oxygen), or are degraded by the conditions encountered
33 in the gastrointestinal tract (digestive enzymes, pH). **These properties can thus affect**
34 **significantly** their bioavailability. The **basis** of encapsulation is to create a biocompatible
35 barrier between the environment and the substance **entrapped** in the protective matrix
36 ([McClements, 2015](#)). Various protection and delivery systems have been proposed to form
37 (micro-)capsules which can release their contents under specific conditions. One well-known
38 strategy is that of trapping bioactive molecules in hydrogel matrices ([McClements, 2017b](#)).
39 Hydrogels are three-dimensional cross-linked networks of natural macromolecules adapted to
40 the controlled release of bioactive compounds due to their sensitivity to environmental
41 stimuli, such as pH and digestive enzymes in the gastrointestinal tract. Proteins, such as dairy
42 or plant proteins, have been **stated as** attractive choices for designing hydrogels **thanks** to their
43 high nutritional value, **their** excellent functional properties and **their** amphiphilic nature
44 **compatible with** many active substances ([Shewan & Stokes, 2013](#)). **Furthermore these**
45 **hydrogels are particularly suitable to entrap hydrophilic compounds thanks to their capacity to**
46 **retain water** ([Aditya et al, 2017](#) ; [McClements, 2017a](#)).

47 Among hydrophilic bioactive molecules, Riboflavin (RF), also known as vitamin B2, is a
48 water-soluble vitamin indispensable for living beings. **It** plays an essential role in energy

49 metabolism of cells and acts as coenzyme factor in various oxidation-reduction processes in
50 cell (Suwannasom et al. 2020). Sufficient dietary or supplemental intake in RF appears to
51 have biological protective effects encompassing anti-oxidant, anti-aging, anti-inflammatory,
52 anti-nociceptive and anti-cancer properties (Suwannasom et al. 2020). However, this molecule
53 of low molar mass (376,36 g/mole) is highly photosensitive and slightly soluble in water
54 (~0.08 g/L at 25 °C) (Morrison et al, 2013 ; Sheraz et al, 2014). Many encapsulation strategies
55 have been proposed in the past 10 years to overcome these drawbacks and to offer
56 nutraceutical solutions. In addition, RF has been chosen as a model molecule in several
57 studies on encapsulation and controlled release of hydrophilic bioactive compounds. Thus, in
58 the recent period authors have investigated the encapsulation of RF in different biopolymeric
59 systems. For instance, particulate systems were proposed such as hydrogel microspheres
60 based on proteins (Chen & Subirade, 2009 ; O'Neill et al, 2014) or sodium alginate (El-
61 Ghaffar et al, 2012 ; Messaoud et al, 2016), dried polysaccharide carriers (de Farias et al,
62 2018 ; Prosapio et al, 2020), or water-in-water emulsions (Chen et al, 2019). Different
63 macromolecular complexes such as inclusion complexes in cyclodextrins (Terekhova et al,
64 2011), protein-polysaccharide electrostatic complexes (Kurukji et al, 2016), β -lactoglobulin-
65 based nanocomplexes (Madalena et al, 2016) or molecularly imprinted polymers (Mokhtari &
66 Ghaedi, 2019), were also investigated. Finally, lipid-based systems such as double emulsions
67 (Bou et al, 2014), liposomes (Ahmad et al, 2015), or solid lipid nanoparticles (Couto et al,
68 2017), were designed. Recently, some authors proposed the use of enzymatically crosslinked
69 plant protein-based hydrogels by using laccase (Yan et al, 2020) or transglutaminase (Wen et
70 al, 2018) for RF encapsulation. In these latter works, encapsulation systems were designed as
71 macrogels, divided in small pieces for release properties evaluation. Assuming that delivery
72 systems usually gain advantages in the form of microparticles, the present paper proposes to
73 design microparticulated hydrogels from crosslinked pea proteins for RF encapsulation.

74 Among plant proteins, pea proteins are considered as good candidates to design encapsulation
75 carrier because of their sustainable production, non-allergenic status and tunable functional
76 properties (Quintero et al, 2018). Furthermore, they have demonstrated good susceptibility to
77 enzymatic crosslinking with transglutaminase, due to their high content in reactive amino acid
78 residues (glutamine and lysine) (Djoullah et al, 2015).

79 In the present work, we evaluated the encapsulation of RF in microparticulated pea protein
80 hydrogels obtained from a double stage process based on the formation of water-in-oil
81 emulsion and subsequent enzymatic gelation of the internal protein phase by using
82 transglutaminase. The emulsification process was first developed to form spherical
83 microparticles of a few tens of micrometers. In a second step, we investigated the in vitro
84 kinetics and release mechanisms of RF in simulated gastric and intestinal fluids.

85 2. Material and methods

86 2.1. Materials

87 Pea flour from yellow peas (*P. sativum* L.) was supplied by Roquette SA (Lestrem, France). A
88 Ca²⁺-independent microbial transglutaminase (MTGase) derived from *Streptoverticillium*
89 *mobarraense* was obtained from Ajinomoto Foods Europe SAS, France. The commercial
90 enzyme preparation (Activia[®] WM) contains 1% active enzyme and 99% maltodextrin. The
91 powdered preparation was assessed to have an activity of 100 U/g. The oily phase (Miglyol
92 812 N) was supplied by Sasol Germany GmbH (Germany). Miglyol is a neutral, colorless,
93 odorless and tasteless edible oil containing medium chain triglycerides. It has a high oxidation
94 stability and remains liquid at 0 °C. Polyglycerol polyricinoleate (PGPR, Grinsted[®] PGPR
95 90, E 476) was obtained from Danisco (Denmark). PGPR is a hydrophobic emulsifier
96 (HLB=1.5±0.5) used for the stabilization of water-in-oil emulsions. Riboflavin, vitamin B2,

97 was supplied by Sigma Aldrich® (France). It is a water-soluble (67-333 mg/L) orange
98 powder. All other chemicals of analytical grade were purchased to VWR International SAS
99 (France) and Sigma–Aldrich® (France).

100 **2.2. Methods**

101 **2.2.1. Pea protein extraction**

102 The extraction of the total pea protein fraction (TPP) was carried out by dispersing 100 g of
103 pea flour in 1 liter of phosphate buffer (0.1 M, pH=8) in the presence of K₂SO₄ 1% for 1 h at
104 4 °C. The protein extract (supernatant) was recovered by centrifugation (12,000g, 10 min)
105 then concentrated (x5) by using an ultrafiltration device (Millipore Pellicon 2®) equipped
106 with a Kwick™ cassette (0.11 m²; 10 kDa cutoff) and operating at 2.2 bar at ambient
107 temperature. The liquid sample was then purified by diafiltration against 10 volumes of a 5
108 mM solution of ammonium carbonate by using the same ultrafiltration device. The pea
109 protein extract obtained was consecutively frozen and lyophilized. The dried protein extract
110 was collected, grinded and stored at -20 °C. The freeze-dried protein isolate had a protein
111 content of 87.2% on a dry basis and a 3.6% water content. The polypeptide profile determined
112 by SDS-PAGE indicated that the protein isolate contained ~20% albumins and ~80%
113 globulins (data not shown).

114 **2.2.2. Microparticle preparation**

115 The pea protein microparticles were prepared by using a microencapsulation process similar
116 to that proposed by Heidebach et al (2009). The procedure consisted in forming a water-in-oil
117 (W/O) emulsion and subsequently applying enzymatic crosslinking for gelling the dispersed
118 protein phase. First, a 15 wt% TPP dispersion was prepared in phosphate buffer (50 mM,
119 pH=7). After 2 h stirring, the MTgase preparation was quickly dispersed in the protein

120 solution at the rate of 20 MTGase U/g protein and the mixture (20 g) was slowly introduced
121 under magnetic stirring (~ 900 rpm) in vials containing 100 g of oil (Miglyol® 812 N)
122 previously heated to 45 °C with or without PGPR. The samples were maintained under
123 stirring during 2 h at 45 °C. After incubation, the dispersed TPP globules were gelled **in the**
124 **form of** microparticles under the action of MTGase. The microparticles were separated from
125 the oil by gentle centrifugation (500g, 5 min), washed twice with 2% Tween 80 solution, then
126 collected on a filter paper and freeze-dried. Alternatively, in order to reduce the size of the
127 microparticles, a thinner emulsion was formed by 5 min homogenization with an Ultra-Turrax
128 (IKA T25) at 10,000 rpm before incubation in the same conditions.

129 **2.2.3. Microparticle size**

130 The size distribution of the microparticles was determined by a Mastersizer 2000 laser
131 granulometer (Malvern Instruments, Southborough, MA). The average size of protein
132 microparticles were calculated as the Sauter mean diameter (d_{32}).

133 **2.2.4. Microscopy**

134 The morphology and external structure of the microparticles were visualized by an optical
135 microscope (Nikon TE2000) equipped with a camera (EMCCO Andor iXon +885).

136 **2.2.5. Microparticle dissolution rate**

137 The dissolution of the microparticles was evaluated in synthetic gastric (HCl solution at
138 pH=1.2) **and intestinal (phosphate buffer at pH=7.4) juices with or without 0.1% pepsin and**
139 **1% pancreatin respectively (Chen and Subirade, 2009)**. For that, 200 mg of freeze-dried
140 microparticles were dispersed in the four digestive fluids (30 ml) with continuous stirring
141 (~100 rpm) at 37 °C. Two ml of supernatant excluding any particles were taken at regular

142 time intervals and the amount of protein was assayed by Kjeldahl method. After each
143 sampling, an equivalent volume of fresh digestive juice was added to maintain a constant
144 volume. The percentage of solubilized microparticles was calculated from Eq.1.

$$145 \quad \% \text{ solubilized microparticles} = (Q_{Pi}/Q_{PT}) * 100 \quad (1)$$

146 where Q_{Pi} is the cumulative amount of dissolved proteins at time i ; Q_{PT} is the amount of
147 proteins after complete microparticle dissolution (10 h).

148 2.2.6. Riboflavin encapsulation

149 The RF encapsulation process was performed as previously described for the preparation of
150 microparticles. RF was introduced into the protein solution at 0.1, 0.5 or 1% concentration
151 before the addition of MTGase. Considering the low solubility of RF powder, the loaded RF
152 in microparticles remained mainly in a crystal form.

153 To evaluate the encapsulation rate of RF in TPP microparticles, encapsulation efficiency (EE)
154 and loading efficiency (LE) were calculated according to the method of Chen and Subirade
155 (2009) with some adaptations. For that, 200 mg of RF-loaded microparticles were dissolved in
156 25 ml of intestinal juice (pH=7.4) with 1% pancreatin at 37 °C under vigorous stirring for 6 h.
157 The mixture was then centrifuged (10,000g, 20 min) and RF was assayed in the supernatant
158 with an UV spectrophotometer (Spectronic BioMate 3) by measuring absorbance at 445 nm
159 and using a calibration curve. EE and LE were calculated by Eqs. 2 and 3 respectively.

$$160 \quad EE = A / B * 100 \quad (2)$$

$$161 \quad LE = A / C * 100 \quad (3)$$

162 where A is the measured amount of RF encapsulated in the sample (mg); B is the theoretical
163 amount of RF corresponding of the initial load in the sample (mg); C is the weight of
164 microparticle sample (mg).

165 **2.2.7. Release kinetics in simulated gastro-intestinal fluids**

166 The RF release kinetics were studied in the gastric and intestinal juices with or without
167 digestive enzymes as proposed by Chen & Subirade (2009) with some modifications. 200 mg
168 of lyophilized microparticles were suspended in 30 ml of each digestive fluid with gentle
169 stirring (~100 rpm) at 37 °C. Two milliliters of supernatant excluding any particles were
170 removed at regular time intervals and then centrifuged (12,000g, 10 min) and the amount of
171 RF in the supernatant was assayed by absorbance measurement at 445 nm. After each
172 sampling, an equivalent volume of fresh digestive juice was added to maintain a constant
173 volume. The percentage of RF released at each time was calculated from Eq. 4.

$$174 \quad \% \text{ of released RF} = (QR_i / QRT) * 100 \quad (4)$$

175 where QR_i is the amount of RF released at time i (mg); QRT is the amount of total RF
176 encapsulated in sample estimated after total dissolution of microparticles (6 h) in the fluid
177 containing digestive enzymes (mg).

178 **2.2.8. Release kinetics modelling**

179 A semi-empirical model, establishing the exponential relationship between the release rate
180 and the time, was used to evaluate the main controlling phenomena. This model known as the
181 Peppas equation (Ritger & Peppas, 1987) represents the release rate as a power law function
182 of time as follows:

$$183 \quad Mt/M_{\infty} = K * t^n \quad (5)$$

184 *where M_{∞} is the amount of active molecule released at the equilibrium (it was assumed that*
185 *total RF release was achieved at an infinite time); M_t is the amount of active molecule*
186 *released over time t ; K is the the release velocity constant, and n is the exponent of release.*

187 **2.2.9. Statistic analysis**

188 All measurements were performed with at least three replicates. The statistical analyses were
189 performed with XLSTAT Pro v2013 software by analysis of variance (ANOVA). A Tukey
190 post-hoc test was used to determine significant differences between group means with a
191 confidence interval of 95% ($p < 0.05$). *Linear regressions and related statistical parameters*
192 *were obtained by using Excel® software (2016, 16.0.5017.1000).*

193 3. Results and discussion

194 3.1. Elaboration and characteristics of microcapsules

195 In order to produce individualized gelled microparticles, a reverse emulsion was first formed
196 by dispersing a 15 wt% TPP suspension containing MTGase in Miglyol oil and incubating the
197 mixture for 2 h at 45 °C. The protein concentration, incubation temperature and time were
198 chosen from preliminary gelation experiments in order to form strong crosslinked protein gels
199 (data not shown). In order to improve the formation of the W/O emulsion, a hydrophobic
200 emulsifying agent (PGPR) was used. Fig. 1 shows light microscopy images of the W/O
201 emulsions after gelation in the absence (Fig. 1a) and in the presence of 1% (Fig. 1b) or 2%
202 (Fig. 1c) PGPR. Without PGPR, the dispersed TPP was gelled in the form of a semi-
203 continuous network composed of interconnected blocks of irregular shape. This could be
204 explained by the poor ability of protein to stabilize reverse emulsion. Proteins are hydrophilic
205 emulsifiers that do not generate W/O interfaces stable enough to prevent the association of
206 TPP globules with each other (Lam & Nickerson, 2013).

207 With 1% PGPR addition (Fig. 1b), the gels were in the form of aggregated microparticles of
208 spherical shape. PGPR is a lipophilic emulsifying agent that facilitate the formation of the
209 W/O interfaces and dispersed globules with regular shape (Zhu et al., 2019). The formation of
210 W/O emulsions generally needs high emulsifying agent concentrations. The 1% PGPR
211 concentration was insufficient to prevent flocculation among microparticles. A higher
212 quantity of PGPR was thus necessary to separate the clustered microparticles. Indeed, the use
213 of 2% of PGPR (Fig. 1c) led to the formation of individual microparticles of spherical shape.
214 Synergistic effect may occur between PGPR and the proteins from the internal phase, that
215 would enhance the efficiency of the lipophilic emulsifying agent (Zhu et al., 2019).

216 The size distribution of the microparticles produced under different conditions were evaluated
217 and typical size profiles are presented in Fig. 2. The microparticles produced in the presence
218 of 1% of PGPR under 900 rpm magnetic agitation had a non-Gaussian and relatively wide
219 distribution with an average diameter of ~320 μm , reflecting a multimodal distribution. This
220 result was consistent with the microscopic observations (Figure 1b) showing that the
221 microparticles gathered in small groups. The size distribution of the systems with 2% and 3%
222 PGPR addition had Gaussian and narrow profiles centered to ~153 and ~149 μm respectively.
223 These microparticle size values were close to those obtained by Heidebach et al. (2009) who
224 used a similar process for encapsulating probiotic cells in MTGase-induced caseinate gels.
225 These sizes cover the main food applications (Heidebach et al., 2009). To produce smaller
226 microparticles, the emulsion was prepared using an Ultra-Turrax homogenizer (5 min, 10,000
227 rpm) with 2% PGPR before incubation. The high-speed homogenization step led to a
228 monomodal size distribution with a ~28 μm average diameter.

229 In the case of food applications, the size of the microcapsules is a determining factor. While
230 large microparticles can change sensory perception, too small microparticles are sometimes
231 unable to offer satisfactory encapsulation capacity. Indeed, the release of the encapsulated
232 molecules is controlled by diffusion phenomena and/or degradation of the matrix, which are
233 generally inversely proportional to the size of the microparticles (Berkland et al., 2002).

234 The degradation of crosslinked TPP-based microparticles was studied in **synthetic** gastric and
235 intestinal fluids **with or without** digestive enzymes at 37 °C. For that, freeze-dried
236 microparticles **resulting** from emulsions prepared using gentle agitation and **with** 2% PGPR,
237 were **assessed**. The dissolution profiles of the microparticles **were** recorded for 10 hours **and**
238 **are reported in** Fig. 3.

239 In the absence of digestive enzymes, the microparticles **were slightly solubilized** (<10%)
240 whatever the pH of the fluid (pH=1.2 and pH=7.4) even up 48 h dissolution (results not
241 shown). **This observation is in agreement with previous works showing the stability of**
242 **MTGase-induced protein microparticles in gastric juice without pepsin (Heidebach et al.,**
243 **2009). Limited particle dissolution** is a desirable feature to control the release of the
244 encapsulated molecules. **Cho et al (2003)** showed **that thermal gels of soy proteins** were 5
245 times more **solubilized** than gels prepared **by enzymatic crosslinking**. This was due to the
246 nature of the bonds stabilizing the protein network, which are covalent in the case of
247 enzymatic crosslinking and mainly non-covalent in the case of thermal gelation.

248 On the other hand, the **addition** of digestive enzymes accelerated the degradation of
249 microparticles (**Fig.3**). The degradation was faster in the intestinal conditions than in the
250 gastric ones. **In the intestinal fluid, the dissolution rate reached 80% and 100% after 90 min**
251 **and 4 h incubation respectively. Under** gastric conditions, the dissolution rate was limited to
252 32% after 90 min and complete dissolution was achieved **after** 10 h. **Smaller degradation of**
253 **microparticles in gastric juice with pepsin in comparison to intestinal conditions was also**
254 **recently reported for similar enzymatically crosslinked protein hydrogels (Wen et al, 2018;**
255 **Yan et al, 2020).** The **observed dissolution** behavior seemed **adapted** to protect the active
256 molecules from the gastric environment and **significantly** release them **during** the intestinal
257 **phase**, as the gastric transit time is typically not longer than 1-2 h (**Gonçalves et al, 2018**).

258 3.2. Riboflavin encapsulation

259 In order to encapsulate RF in the microparticles, RF was dispersed in the TPP solution before
260 emulsification. Three RF contents (0.1, 0.5 and 1.0 wt%) in the protein solution were studied
261 to assess the loading capacity of the microparticles. The microcapsules were prepared from
262 W/O emulsions containing 2% PGPR using magnetic agitation only or with pre-
263 homogenization by Ultra-Turrax. The encapsulation efficiency (EE) as well as the loading
264 efficiency (LE) of the microparticles are reported in Table 1. The size of the loaded
265 microparticles resulting from mild agitation condition was close to 150 μm whatever the RF
266 concentration. The size of the microparticles prepared with high-speed homogenization was
267 significantly lower ($\sim 32 \mu\text{m}$) in agreement with the previous observations (section 3.1). For
268 the largest microparticles, the EE values decreased significantly from $\sim 84\%$ to $\sim 74\%$ when
269 increasing RF concentration, while the smallest microparticles had the lowest EE ($\sim 56\%$).
270 The same trends were logically observed for LE values. The microparticle size variation from
271 ~ 150 to $\sim 30 \mu\text{m}$, following the use of high-speed homogenization, resulted in one-third
272 decrease of LE and EE values. The EE values were in the same order of magnitude as those
273 found by Chen et al. (2007) for RF encapsulation in alginate-whey protein microparticles
274 generated from an emulsification and internal gelation process. The decrease in EE was
275 mainly explained by the size of the RF crystals relative to the microparticle size. This
276 behavior was confirmed by microscopic observations of loaded microparticles (Fig. 4). It was
277 clearly observed that the larger microparticles (Fig. 4a) are significantly better suited for
278 incorporating large RF crystals than the smaller microparticles (Fig. 4b). These observations
279 were again consistent with the findings of Chen et al (2007) for alginate-whey protein
280 microspheres ($<100 \mu\text{m}$) encapsulating RF crystals. Typically, RF solubility vary between a
281 few mg/L and a few tens of mg/L depending on the crystal form, the solvent temperature and
282 pH (Rivlin, 2012). Owing to its low solubility, RF remained mainly crystallized in the form of

283 “short thin needles” (5 to 10 μm) in the TPP microparticles after encapsulation. Because of
284 these particular shape and size, the RF crystals were not totally incorporated in 30 μm
285 microparticles. Part of the RF flakes remaining outside the microparticles would be then
286 dissolved and/or removed by the washing step after enzymatic incubation.

287 3.3. Release kinetics and mechanism

288 The microparticles produced from W/O emulsion by applying magnetic stirring at 1% RF
289 concentration were chosen for further release experiments. The release kinetics of RF from
290 the loaded microparticles was carried out at 37 $^{\circ}\text{C}$ in four different fluids: pH=1.2; pH=1.2 +
291 pepsin; pH=7.4 and pH=7.4 + pancreatin for 6 hours. The corresponding results are presented
292 in Fig. 5.

293 The release of RF was enhanced by the addition of digestive enzymes in both gastric and
294 intestinal juices. RF release evolved faster under intestinal conditions (pH=7.4 + pancreatin)
295 than under gastric ones (pH=1.2 + pepsin). Complete release of RF (100%) was achieved after
296 4 and 6 h respectively. These release profiles were very similar to those observed for the
297 dissolution experiments (Fig. 3) in intestinal conditions but slightly different in the case of
298 gastric conditions since the degradation was longer in the latter case. The present release
299 behaviours reflected probably different phenomena such as mainly matrix degradation,
300 solubilization of crystallized RF and/or its diffusion. As shown in Fig. 4C at a microscopic
301 scale, the surface of TPP microparticles were early degraded in the intestinal juice with
302 pancreatin, whereas the peripheral RF crystals became exposed. The gradual release of RF
303 from the outer layers to the inner layers due to the proteolytic action of pancreatin could be
304 thus hypothesized.

305 In the absence of digestive enzymes, RF release rates evolved **much** more slowly
306 **independently** of digestive conditions (pH=1.2; pH=7.4), reaching only a 40% value after 6 h.
307 The release profiles differed in intensity from those observed under the same conditions for
308 microparticle dissolution since the degradation rate **remained below** 10% in the latter case
309 (Fig. 3). This could indicate that diffusion phenomena predominated in the case of limited
310 microparticle degradation.

311 The release mechanisms of active molecules from polymeric matrices are generally based on
312 two main phenomena: degradation (dissolution **or** erosion) of the encapsulating support and
313 diffusion of the active molecule through the support; but other phenomena have to be taken
314 into account such as swelling, glass transition, chemical degradation, osmotic effect or
315 reaction. (Peppas & Narasimhan, 2014). Many mathematical models have been proposed to
316 simulate the release kinetics of encapsulated agents from hydrogel-**based** systems (Lin &
317 Metters, 2006, Peppas & Narasimhan, 2014). In the present paper, the Peppas equation (Eq. 5)
318 was used in order to distinguish between the main controlling phenomena. This **power law**
319 model is generally applicable for the first ~60% of the release profile (Lin & Metters, 2006),
320 so that it was applied to release rate values below 70% in a logarithmic representation for all
321 the **experimental** release kinetics (Fig. 6). Thus, the n value corresponded to the slope of the
322 interpolating straight line for each release condition. The experimental values of n as well as
323 the regression coefficients (R^2) were reported Table 2.

324 All the regression coefficients were found higher than ~0.96 indicating the appropriateness of
325 the model to fit the data. The n values **varied** between 0.48 and 0.81 **and were** compared to **the**
326 **theoretical values corresponding to** Fickian and non-Fickian transport behaviours (Ritger &
327 Peppas, 1987). In a pure Fickian model (Case I), $n = 0.45$ for a spherical geometry and the
328 active molecule release is governed by diffusion. The exponent values calculated for the

329 simulated gastric and intestinal fluids without digestive enzyme were 0.48 and 0.51
330 respectively, close to the theoretical value for diffusion behaviour. The discrepancy
331 observed between experimental and theoretical values could be explained by a limited
332 dissolution effect (<10% degradation rate) and other phenomena like swelling or
333 heterogeneous particle size distribution, that may influence diffusion kinetics (Ritger &
334 Peppas, 1987). In the present case, progressive solubilization of RF crystals inside
335 microparticles accompanied also diffusion of RF molecules through the crosslinked protein
336 network.

337 A pure erodible system corresponds generally to a zero-order release kinetics (Lin et al.,
338 2006). In this case, the amount of active substance released is proportional to time ($n=1$) for a
339 system with a constant planar surface as a slab-shaped geometry. It could be assimilated to the
340 Case II condition of the power law model for which $n=0.85$ for a spherical geometry even if
341 this case is generally related to relaxation of the polymeric matrix (Ritger & Peppas, 1987).
342 The n value determined for intestinal fluid with added pancreatin ($n = 0.81$) was close to this
343 value, indicating the RF release was mainly controlled by the enzymatic degradation of the
344 protein microparticles. The release exponent calculated for the gastric fluid with pepsin was
345 0.6 indicating an intermediary behaviour as the dissolution of TPP microparticles was
346 significantly slower compared to intestinal conditions. In agreement with these results,
347 comparable systems based on enzymatically crosslinked protein hydrogels (Wen et al, 2018;
348 Yan et al, 2020) have shown non-Newtonian RF release behaviour under gastric conditions
349 and erosion-controlled behaviour under intestinal conditions. The choice to test the
350 microparticles in the gastric and intestinal artificial juices separately, made it possible to
351 clearly identify the behavior of our system for each digestive condition. Extrapolated to real
352 digestive conditions, the present results suggested that RF could be regularly released up to
353 ~40-50% during the gastric phase (<90 min), likely followed by a very fast release of the

354 remaining RF from the pre-degraded protein microparticles **under** intestinal conditions.
355 **Sequential and standardized in vitro digestion protocol such as the INFOGEST method**
356 **(Minekus et al., 2014) would be necessary to validate these synergistic release effects.**

357 **4. Conclusion.**

358 Pea protein microparticles encapsulating **RF** were successfully prepared by W/O emulsion
359 and enzymatic gelation. The size of the microparticles (~150 µm) was controlled by mild
360 agitation during emulsion preparation and adequate concentration of the hydrophobic
361 emulsifying agent. This size was adapted to entrap **RF** crystals with a significant yield
362 (>74%). The release of **RF** from the enzymatically crosslinked microparticles seemed
363 controlled by diffusion in digestive juices when no proteolytic enzyme was added. In the
364 presence of digestive enzymes, the release kinetics could correspond to erosion-like behaviour
365 **under** intestinal conditions and intermediary situation **under** gastric **conditions** where diffusion
366 and matrix degradation occurred simultaneously. The protein microparticles would thus
367 ensure a sufficient protection of **RF** to allow significant release during intestinal phase. This
368 **conclusion needs further validation** by applying successive digestive steps or **using a**
369 **continuous-type digester.**

370 **Acknowledgement**

371 Authors are grateful to Ajinomoto Foods Europe SAS for providing the MTGase powder and
372 to Conseil Régional de Bourgogne (France) for its financial support (PARI MATBIO).

373 **References**

374 Aditya, N.P., Espinosa, Y.G., & Norton, I.T. (2017). Encapsulation systems for the delivery
375 of hydrophilic nutraceuticals: Food application. *Biotechnology Advances*, 35(4), 450-457.

376 Ahmad, I., Arsalan, A., Ali, S.A., Sheraz, M.A., Ahmed, S., Anwar, Z., Munir, I., & Shah,
377 M.R. (2015). Formulation and stabilization of riboflavin in liposomal preparations. *Journal of*
378 *Photochemistry and Photobiology B: Biology*, 153, 358-366.

379 Berkland, C., King, M., Cox, A., Kim, K.K., & Pack, D.W. (2002). Precise control of PLG
380 microsphere size provides enhanced control of drug release rate. *Journal of Controlled*
381 *Release*, 82(1), 137-147.

382 Bou, R., Cofrades, S., & Jiménez-Colmenero, F. (2014). Physicochemical properties and
383 riboflavin encapsulation in double emulsions with different lipid sources. *LWT - Food Science*
384 *and Technology*, 59(2), 621-628.

385 Chen, J.F., Guo, J., Liu, S.H., Luo, W.Q., Wang, J.M., & Yang, X.Q. (2019). Zein particle-
386 stabilized water-in-water emulsion as a vehicle for hydrophilic bioactive compound loading of
387 riboflavin. *Journal of Agricultural and Food Chemistry*, 67(35), 9926-9933.

388 Chen, L., & Subirade, M. (2007). Effect of preparation conditions on the nutrient release
389 properties of alginate–whey protein granular microspheres. *European Journal of*
390 *Pharmaceutics and Biopharmaceutics*, 65(3), 354-362.

391 Chen, L., & Subirade, M. (2009). Elaboration and characterization of soy/zein protein
392 microspheres for controlled nutraceutical delivery. *Biomacromolecules*, 10(12), 3327-3334.

393 Cho, Y.H., Shim, H.K., Park, J., (2003). Encapsulation of fish oil by an enzymatic gelation
394 process using transglutaminase cross-linked proteins. *Journal of Food Science*, 68(9), 2717-
395 2723.

396 Couto, R., Alvarez, V., & Temelli, F. (2017). Encapsulation of Vitamin B2 in solid lipid
397 nanoparticles using supercritical CO₂. *The Journal of Supercritical Fluids*, 120, 432-442.

398 de Farias, S. S., Siqueira, S. M. C., Cunha, A. P., de Souza, C. A. G., dos Santos Fontenelle,
399 R.O., de Araújo, T.G., de Amorim, A.F.V., de Menezes, J.E.S.A., Morais, S.M., & Ricardo,
400 N.M.P.S. (2018). Microencapsulation of riboflavin with galactomannan biopolymer and
401 F127: Physico-chemical characterization, antifungal activity and controlled release. *Industrial*
402 *Crops and Products*, 118, 271-281.

403 Djoullah, A., Djemaoune, Y., Husson, F., & Saurel, R. (2015). Native-state pea albumin and
404 globulin behavior upon transglutaminase treatment. *Process Biochemistry*, 50(8), 1284-1292.

405 Đorđević, V., Balanč, B., Belščak-Cvitanović, A., Lević, S., Trifković, K., Kalušević, A.,
406 Kostić, I., Komes, D., Bugarski, B., & Nedović, V. (2015). Trends in encapsulation
407 technologies for delivery of food bioactive compounds. *Food Engineering Reviews*, 7(4), 452-
408 490.

409 El-Ghaffar, M.A., Hashem, M.S., El-Awady, M.K., & Rabie, A.M. (2012). pH-sensitive
410 sodium alginate hydrogels for riboflavin controlled release. *Carbohydrate Polymers*, 89(2),
411 667-675.

412 Gonçalves, R.F., Martins, J.T., Duarte, C.M., Vicente, A.A., & Pinheiro, A.C. (2018).
413 Advances in nutraceutical delivery systems: From formulation design for bioavailability
414 enhancement to efficacy and safety evaluation. *Trends in Food Science & Technology*, 78,
415 270-291.

416 Heidebach, T., Först, P., & Kulozik, U. (2009). Transglutaminase-induced caseinate gelation
417 for the microencapsulation of probiotic cells. *International Dairy Journal*, 19(2), 77-84.

418 Kurukji, D., Norton, I., & Spyropoulos, F. (2016). Fabrication of sub-micron protein-chitosan
419 electrostatic complexes for encapsulation and pH-Modulated delivery of model hydrophilic
420 active compounds. *Food Hydrocolloids*, 53, 249-260.

421 Lam, R.S.H., & Nickerson, M.T. (2013). Food proteins: A review on their emulsifying
422 properties using a structure–function approach. *Food Chemistry*, 141(2), 975–984.

423 Lin, C.C., & Metters, A.T. (2006). Hydrogels in controlled release formulations: network
424 design and mathematical modeling. *Advanced Drug Delivery Reviews*, 58(12-13), 1379-1408.

425 Madalena, D.A., Ramos, Ó.L., Pereira, R.N., Bourbon, A.I., Pinheiro, A.C., Malcata, F.X., &
426 Vicente, A.A. (2016). In vitro digestion and stability assessment of β -lactoglobulin/riboflavin
427 nanostructures. *Food Hydrocolloids*, 58, 89-97.

428 McClements, D.J. (2015). Encapsulation, protection, and release of hydrophilic active
429 components: potential and limitations of colloidal delivery systems. *Advances in Colloid and*
430 *Interface Science*, 219, 27-53.

431 McClements, D.J. (2017a). Designing biopolymer microgels to encapsulate, protect and
432 deliver bioactive components: Physicochemical aspects. *Advances in Colloid and Interface*
433 *Science*, 240, 31-59.

434 McClements, D.J. (2017b). Recent progress in hydrogel delivery systems for improving
435 nutraceutical bioavailability. *Food Hydrocolloids*, 68, 238-245.

436 Messaoud, G.B., Sánchez-González, L., Probst, L., Jeandel, C., Arab-Tehrany, E., & Desobry,
437 S. (2016). Physico-chemical properties of alginate/shellac aqueous-core capsules: Influence of
438 membrane architecture on riboflavin release. *Carbohydrate Polymers*, 144, 428-437.

439 Minekus, M., Alming, M., Alvito, P., Ballance, S., Bohn, T., Bourlieu, C., Carrière, F.,
440 Boutrou, R., Corredig M., Dupont, D., Dufour, C., Egger, L., Golding, M., Karakaya, S.,
441 Kirkhus, B., Le Feunteun, S., Lesmes, U., Macierzanka, A., Mackie, A., Marze, S.,
442 McClements, D.J., Ménard, O., Recio, I., Santos, C.N., Singh R.P., Vegarud, G.E., Wickham,

443 M.S.J., Weitschies, W., & Brodkorb, A. (2014). A standardised static in vitro digestion
444 method suitable for food—an international consensus. *Food & Function*, 5(6), 1113-1124.

445 Mokhtari, P., & Ghaedi, M. (2019). Water compatible molecularly imprinted polymer for
446 controlled release of riboflavin as drug delivery system. *European Polymer Journal*, 118,
447 614-618.

448 Morrison, P.W., Connon, C.J., & Khutoryanskiy, V.V. (2013). Cyclodextrin-mediated
449 enhancement of riboflavin solubility and corneal permeability. *Molecular Pharmaceutics*,
450 10(2), 756-762.

451 O'Neill, G.J., Egan, T., Jacquier, J.C., O'Sullivan, M., & O'Riordan, E.D. (2014). Whey
452 microbeads as a matrix for the encapsulation and immobilisation of riboflavin and peptides.
453 *Food Chemistry*, 160, 46-52.

454 Peppas, N.A., & Narasimhan, B. (2014). Mathematical models in drug delivery: How
455 modeling has shaped the way we design new drug delivery systems. *Journal of Controlled*
456 *Release*, 190, 75-81.

457 Prosapio, V., Norton, I.T., & Lopez-Quiroga, E. (2020). Freeze-dried gellan gum gels as
458 vitamin delivery systems: modelling the effect of pH on drying kinetics and vitamin release
459 mechanisms. *Foods*, 9(3), 329.

460 Quintero, J., Rojas, J., & Ciro, G. (2018). Vegetable proteins as potential encapsulation
461 agents: a review. *Food Research*, 2(3), 208-220.

462 Ritger, P. L., & Peppas, N. A. (1987). A simple equation for description of solute release I.
463 Fickian and non-fickian release from non-swellable devices in the form of slabs, spheres,
464 cylinders or discs. *Journal of Controlled Release*, 5(1), 23-36.

465 Sheraz, M. A., Kazi, S. H., Ahmed, S., Anwar, Z., & Ahmad, I. (2014). Photo, thermal and
466 chemical degradation of riboflavin. *Beilstein Journal of Organic Chemistry*, 10(1), 1999-
467 2012.

468 Shewan, H.M., & Stokes, J.R. (2013). Review of techniques to manufacture micro-hydrogel
469 particles for the food industry and their applications. *Journal of Food Engineering*, 119(4),
470 781-792.

471 Suwannasom, N., Kao, I., Pruß, A., Georgieva, R., & Bäumlér, H. (2020). Riboflavin: The
472 health benefits of a forgotten natural vitamin. *International Journal of Molecular Sciences*,
473 21(3), 950.

474 Terekhova, I.V., Tikhova, M.N., Volkova, T.V., Kumeev, R.S., & Perlovich, G.L. (2011).
475 Inclusion complex formation of α - and β -cyclodextrins with riboflavin and alloxazine in
476 aqueous solution: thermodynamic study. *Journal of Inclusion Phenomena and Macrocyclic*
477 *Chemistry*, 69(1-2), 167-172.

478 Wen, X., Jin, F., Regenstein, J.M., & Wang, F. (2018). Transglutaminase induced gels using
479 bitter apricot kernel protein: Chemical, textural and release properties. *Food Bioscience*, 26,
480 15-22.

481 Yan, W., Zhang, B., Yadav, M.P., Feng, L., Yan, J., Jia, X., & Yin, L., (2020), Corn
482 fibergum-soybean protein isolate double network hydrogel as oral delivery vehicles for
483 thermosensitive bioactive compounds, *Food Hydrocolloids*, doi:
484 <https://doi.org/10.1016/j.foodhyd.2020.105865>.

485 Zhu, Q., Pan, Y., Jia, X., Li, J., Zhang, M., & Yin, L. (2019). Review on the stability
486 mechanism and application of water-in-oil emulsions encapsulating various additives.
487 *Comprehensive Reviews in Food Science and Food Safety*, 18(6), 1660-1675.

Figure 1 : Light microscopy images of the TPP microparticles in absence or presence of emulsifying agent : (a) without PGPR; (b) with 1% PGPR; (c) with 2% PGPR (d) with 2% PGPR and applying Ultra-Turrax homogenization.

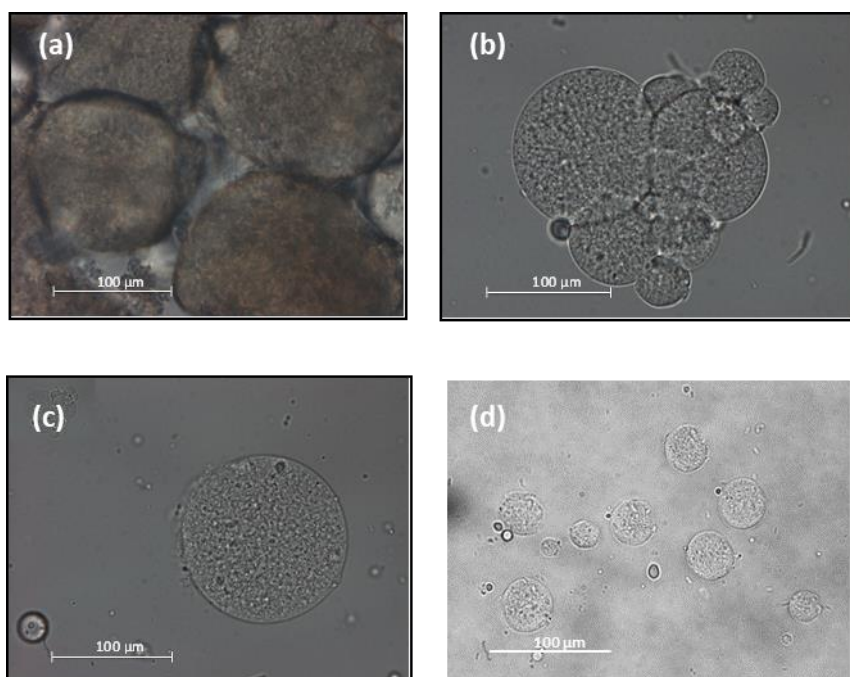


Figure 2: Size distribution of crosslinked TPP microparticles prepared with different emulsifying agent (PGPR) concentrations and different emulsifying conditions.

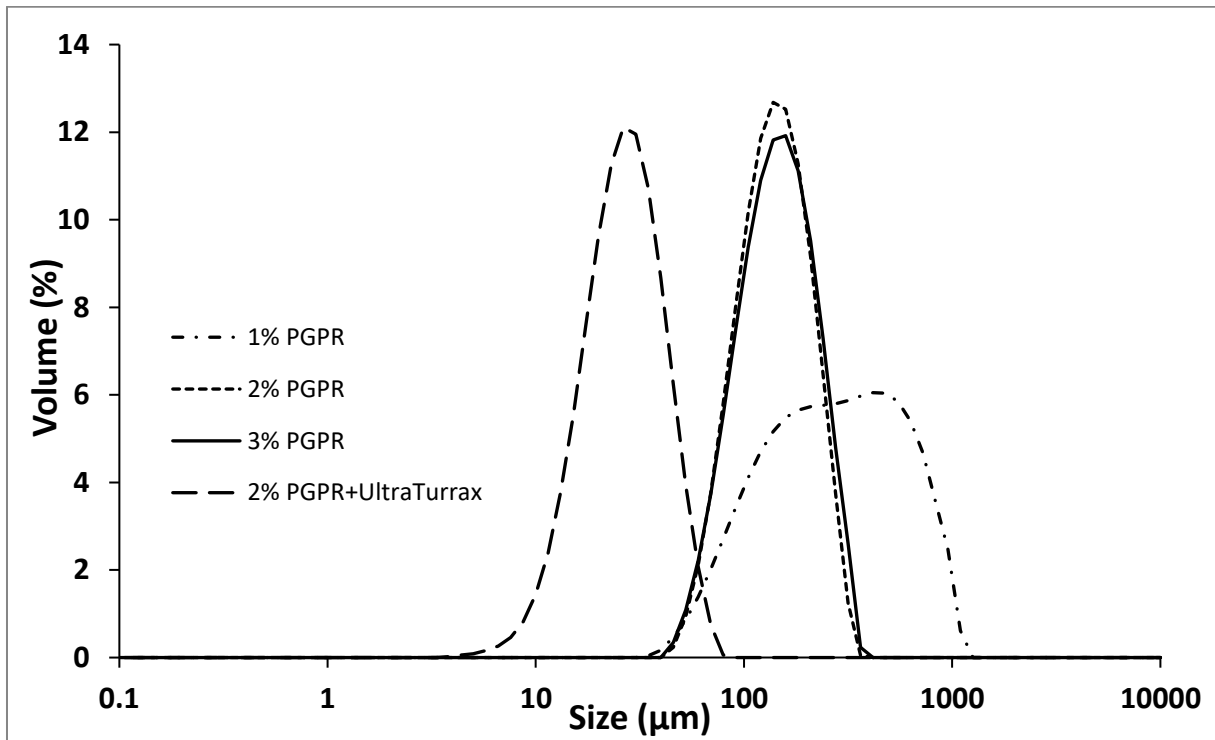


Figure 3 : Dissolution rate of TPP microparticules under gastric (pH 1.2 ; pH 1.2 + pepsin) and intestinal conditions (pH 7.4 ; pH 7.4 + pancreatin) at 37 °C.

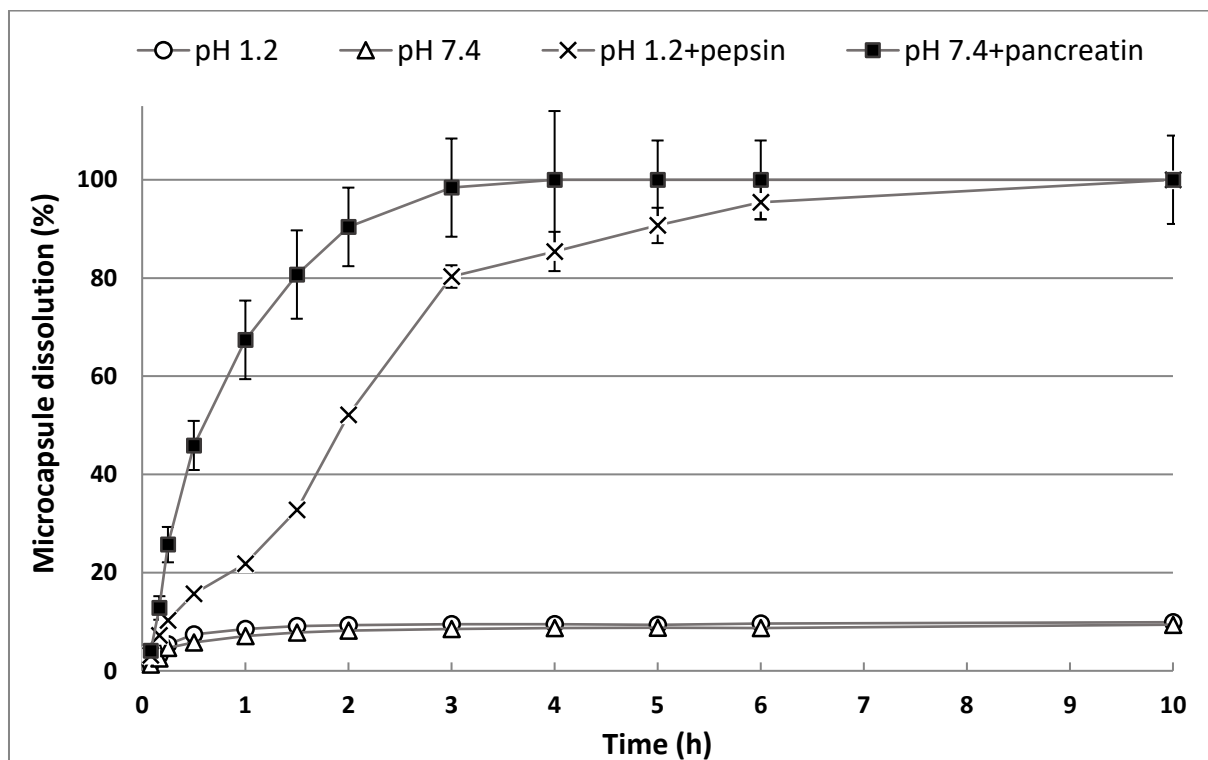


Figure 4 : Light microscopy images of the RF-loaded microparticles prepared by magnetic agitation (a) or by Ultra-Turrax homogenization (b); microparticle after 5 minutes in the intestinal fluid with pancreatin (c). **RF crystal appeared in yellow-orange.**



Figure 5 : Release kinetics of riboflavin from microparticles in different simulated digestive fluids at 37 °C.

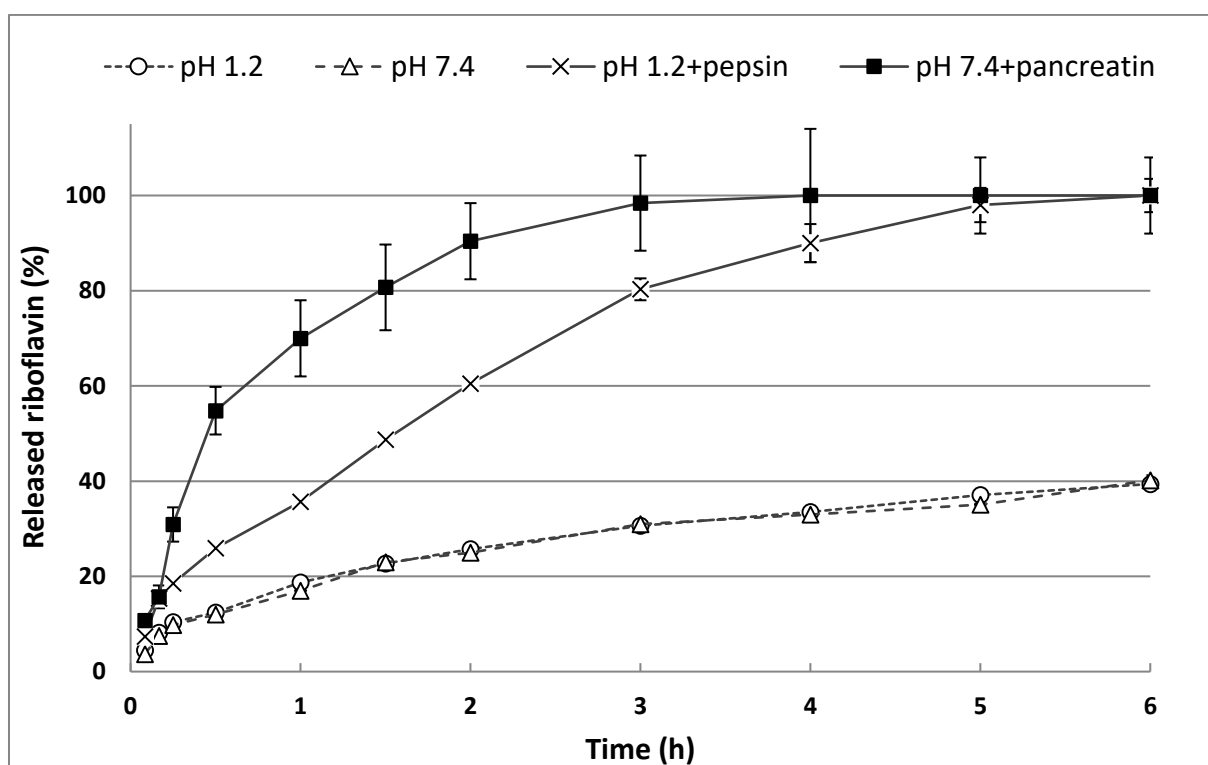


Figure 6 : Logarithmic representation of the release kinetics according to the power law model (Ritger & Peppas, 1987). Points : experimental data. Dashed straight lines : adjusted linear models.

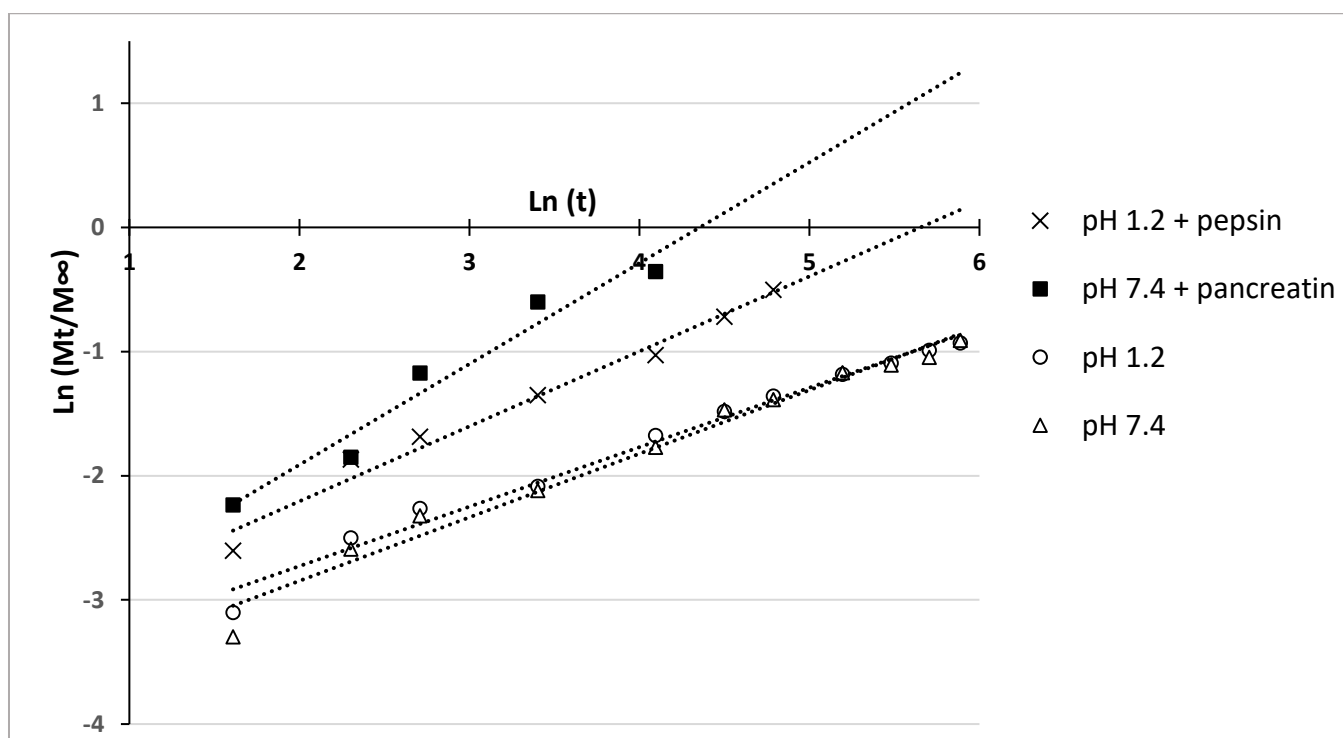


Table 1 : Mean diameter (d_{32}), **encapsulation efficiency (EE)** and **loading efficiency (LE)** of microparticules prepared with different emulsification methods and at different riboflavin contents (C_{Ribo}).

C_{Ribo} (%)	Agitation (rpm)	d_{32} (μm)	EE (%)	LE (%)
0.1	900	149.2 ± 1.8^a	84.1 ± 2.4^a	0.56 ± 0.02^a
0.5	900	148.4 ± 2.9^a	81.7 ± 2.6^a	2.72 ± 0.09^b
1.0	900	151.6 ± 3.1^a	74.5 ± 3.4^b	4.97 ± 0.23^c
0.1	+10000 (Ultra-Turrax)	31.7 ± 1.2^b	56.5 ± 3.4^c	0.38 ± 0.02^d

Different superscripts in the same column represent significant differences ($p < 0.05$) among samples

Table 2 : Release exponent values (n) and regression coefficient (R^2) of the power law model from different release kinetics.

Release fluids	n	R^2
pH 1.2	0.48 ± 0.07^a	0.986
pH 1.2 + pepsin	0.60 ± 0.03^b	0.956
pH 7.4	0.51 ± 0.02^a	0.978
pH 7.4 + pancreatin	0.81 ± 0.02^c	0.979

Different superscripts in the same column represent significant differences ($p < 0.05$) among samples